Research Article

Role of Relativistic Quantum Theory in Hadron Radiation Therapy

M.G.Shabankareh[a],S.N. Hosseinimotlagh[a], N. Farhangkhah[a]

a Department of Physics, Shiraz Branch, Islamic Azad University, Shiraz, Iran

*** Corresponding author Email: nasrinhosseinimotlagh@gmail.com**

DOI: 10.30495/ijbbe.2023.1980428.1024

ABSTRACT

Received: Feb. 23, 2023, Revised: May. 19, 2023, Accepted: Jul. 18, 2023, Available Online: Jul. 30, 2023

In recent years, the attention of scientists has been drawn to laser accelerators because they have a smaller size and more power than RT accelerators. But to upgrade these laser accelerators for hadron therapy, the theory governing these accelerators needs more investigation. The present paper represents the theory of laser-driven accelerators. Also, for the first time, we calculated the quantum relativistic important parameters such as the effective atomic number, z_{eff}, $\beta = {}^{v}/_{c}$, parameter, the density effect, ${}^{\delta}/_{2}$, the shell effect,ΔL_{shell}, Barkas effect, L_{Barkas} , Lynard Sorensen, effect, ΔL_{LS}, the standard perturbation function, L_{stand}, the first order general term of quantum perturbation theory, L_{Pert}, for proton and carbon beams in different energies versus the depth of penetration in the different human tissues using Maple programming, and our numerical results show that since the physical and chemical properties of carbon and hydrogen ions are not the same and carbon is heavier than hydrogen, carbon and hydrogen ion beams in hadron therapy do not have the same behavior inside the different human tissues.

KEYWORD

carbon, proton, laser, relativistic, tissues, quantum.

I. INTRODUCTION

In 1952, human patients were first treated with beams of particles such as deuterons and helium by Cornelius Tobias and John Lawrence [1]. After that, with the emergence of proton facilities in the world, interest in using particle beams to treat patients developed. As the biological effect of proton beams was reflected compared to X-rays, researchers found a tendency towards heavier ions due to higher biological effects as well as higher linear energy transfer [2]. In 1975, with the installation of BEVALAC at the Lawrence Berkeley Laboratory, extensive research into the clinical feasibility of heavy ion beam therapy officially began [3]. Following initial successes at Lawrence Berkeley Lab, in 1984, the Japanese government began construction of the world's first heavy ion facility for medical use at the National Institute of Radiological Sciences. Construction of the heavy ion `medical accelerator in Chiba was completed

in 1993, and clinical trials of carbon ion beam therapy (C-ion RT) began in June 1994.

The use of radiation therapy is based on achieving precise localization of the dose in the desired target and causing minimal damage to the surrounding healthy tissues. The energy transfer of carbon ion beams to the tissue is maximized in the last few millimeters of their range, this maximum is called the Bragg's peak, since the main peak is very narrow and sharp to completely cover the cancerous tissue, the spread-out Bragg peak is used in cancer treatment according to the size of the tissue [4,5]. This allows carbon ion beams to provide highly localized deposited energy and be used to increase the radiation dose to tumors while minimizing radiation to adjacent healthy tissues. Proton therapy also has this feature. However, lateral collapsing of tissues around the target occurs faster with carbon ion beams than with proton beams. In the region beyond the distal end of the peak, almost no dose is deposited with protons, while a small dose is deposited with carbon ions. This is because the primary carbon ions undergo nuclear interactions and decay into particles. They transform with a lower atomic number and create a fragmentation sequence beyond the peak [4]. Radiation therapy damages the DNA of cancer cells. X-rays often break single-stranded DNA, while breaking double-stranded DNA with two hits is inevitable for the death of cancer cells. It is important to note that cells have mechanisms to repair single-stranded DNA damage, and some may survive even after treatment. Carbon ion beams provide more average energy per unit length of linear energy transfer of their path through the body compared to low linear energy transfer radiations such as protons or photons. Consequently, carbon ion beams, which are high linear energy transfer radiation, usually cause single-impulse DNA double-strand breaks, which is the most important event for cancer cell death [5].

In linear energy transfer to evaluate the biological effects of radiation, it is used the fact that the relative biological effectiveness increases with the increase of linear energy transfer [6-7]. Studies show that the linear energy transfer of carbon ion beams continuously increases from the point of radiation in the body with increasing depth to reach its maximum value at the Bragg peak. When carbon ion beams are used in cancer treatment for deep tumors, this property becomes a therapeutic advantage. Compared to protons or X-ray beams, linear energy transfer of heavy ions has various biological advantages, including reduction of oxygen enhancement ratio, reduction of cell cycle-dependent radiosensitivity, potential suppression of metastases, and effectiveness of cancer stem cells [8-11]. These properties offer the advantage of using heavy ion beams in the treatment of tumors such as adenocarcinoma, adenoid cystic carcinoma, malignant melanoma, and sarcoma, which are very resistant to low radiation and sometimes cannot be controlled even by simple dose increases. When fast ions pass through matter, their deposited energy is roughly due to interactions with and transfer of energy to electrons. In this paper, we study the stopping power corresponding to light and heavy ions when their speed approaches the speed of light.

In order to be able to use particle beams with high energy to treat all types of cancer, we must accelerate the charged particles by accelerators. Today, electron (ion) accelerators, which are accelerated by laser pulse propagation in a plasma environment, have attracted a lot of attention in the technology of particle accelerators [7-9]. Laser-plasma accelerators are amazing in terms of power and have sufficient energy band, pulse duration, and sufficient peak dose rate in comparison with other accelerators, and in the meantime, they can have a better dose delivery and higher acceleration in particle therapy in more effective cancer treatment. Laser-plasma accelerators of charged particles are compact, simple, and low-cost accelerators. Therefore, they can be easily placed in the basements of existing hospitals. Since the treatment of cancer is one of the major challenges in today's world and there is still no completely safe and cost-effective way to eradicate this disease, it is

hoped that by using high-energy hadrons accelerated by a laser, promising results can be achieved. The goal of the authors of this article has been achieved for the first time to investigate the theory of hadron therapy of tumors by irradiation with proton and carbon beams with high relativistic energy through the numerical solution of the Bethe-Bloch stopping power formula for several different tumors and comparing the results obtained with the works of other groups. Research is available. Therefore, this article is organized as follows:

In Section 2, we introduce nuclear interactions between light and heavy ions. In Section 3, the theoretical quantum relativistic stopping power and range for hadrons such as protons and carbons in human tissues is presented. In sections 4 and 5, important parameters such as absorbed dose, energy, and amplitude reduction are described, respectively. Finally, the conclusion is presented.

II. NUCLEARINTERACTIONS

Charged particles can also interact with material nuclei through nuclear interactions. These interactions are significantly less involved in energy loss than electromagnetic processes. Unlike electromagnetic interactions, there is no exact model to describe them. In the following, we briefly describe common approaches to modeling nuclear interactions.

General aspects:
Nuclear interactions are performed in two separate steps. First, the probability of a nuclear event is sampled based on the nuclear cross-section. Depending on the particle and its incident energy, these can be calculated "on the flight". Nuclear interactions (collision) can be divided into the following:

Elastic Collision:
Here the kinetic energy remains constant and the nucleus remains intact. This is similar to Coulomb multiple scattering, but it is due to strong interactions and not electromagnetic interactions. Such interactions do not happen very often.

Inelastic collisions:

Here a more violent reaction occurs between the projectile and the target where the total kinetic energy does not remain constant. The projectile may eject secondary particles (protons, neutrons, deuterons, etc.) from the nucleus and become fragments if they are ions. The probability of no nuclear interaction P(x) after traveling a distance x in a substance is given by : $P(x) = \frac{N(x)}{N(0)} = e^{\frac{-x}{\lambda_{int}}}$. Where N is the number of incident particles, $N(x)$ is the number of particles after traveling the distance x, λ_{int} is the mean free path or interaction length, which is defined by: $\lambda_{int} = \frac{A_t}{N_A \sigma \rho}$ and where σ is the total cross-section. Since there are important differences in the modeling of nuclear interactions for protons and heavy ions, we discuss them separately [12,13].

A. *Nuclear interactions of protons*

It is usually assumed that a proton hitting the atomic nucleus initiates a series of nucleon-nucleon collisions that result in the emission of protons, neutrons, and light fragments, thereby balancing the rest of the nucleus. This process can be described as a three-step sequence [14, 15], which is shown schematically in Fig.1 and the upper part of Fig. 2.

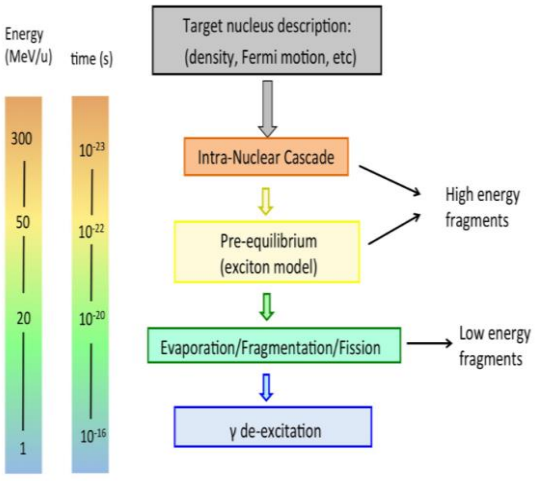

Fig. **1** Schematic representation of the stages of a nucleus-nucleon interaction related to radiation therapy, along with the time scale and energy of the interacting particles.

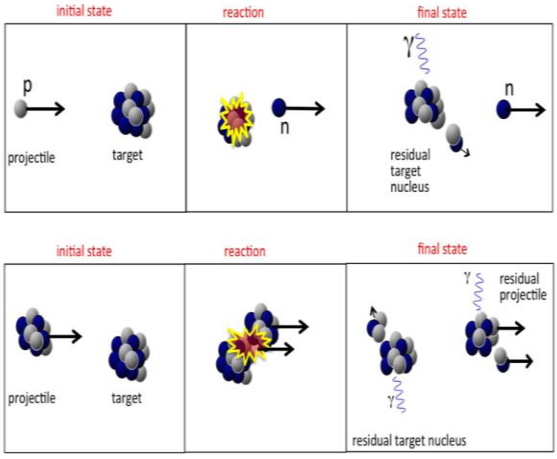

Fig. **2** Top: Schematic of a possible nucleon-nucleus reaction in proton therapy, whereby neutrons are produced. Bottom: Schematic of nuclear-nuclear reaction with heavy ion therapy, with the creation of fragments.

Intra-Nuclear Cascade (INC): this model is usually used to describe the nuclear interactions of nucleons with energy above 50 MeV to hundreds of GeV, which was originally investigated by Serber and Heisenberg [16]. The basic idea is that the incident particle interacts with meta-free nucleons in the target nucleus through a series of two-body interactions. The target nucleus is modeled as a Fermi gas of cold and free nucleons. The nucleons inside this nuclear environment are accounted for by the nuclear density distribution, the nuclear potential, and the Pauli exclusion principle. This "free" nucleon method is justified if the wavelength of the incident particle is much smaller than the average distance between nucleons in the nucleus of matter and is much smaller than the mean free path inside the nucleus.

It turns out that the INC model surprisingly works at much lower energy than expected, thanks to quantum effects such as the Pauli exclusion principle, nucleon-nucleon correlations, etc., effective mean free path of nucleons in the nuclear environment increase. For proton therapy energies only elastic scattering occurs because these energies are below the pion production threshold (290 MeV).

The final product particles resulting from the scattering process are called secondary particles. Their production time in the time scale of strong interactions is $10^{-23}s$ to $10^{-22}s$. Secondary particles have a lot of energy and can re-scatter on the same nucleus or escape, etc. Not only protons and neutrons can be emitted, but they can also be produced through the coagulation mechanism of light nuclear fragments with high energy. All particles are tracked until all are below a certain energy threshold, usually a few tens of MeV. This process is called an intra-nuclear cascade. The description of this process is very complex, because all secondary particles must be properly transported through the nuclear medium and require a detailed description of the nuclear density, quantum effects, nuclear potential, binding energy, Fermi motion, etc, [17,18].

Pre-equilibrium: At this stage, the energy of the particles in the cascade reaches a lower limit, usually a few tens of MeV, but the nucleus is still not in thermal equilibrium. The evolution of the nuclear reaction is also represented as successive nucleon-nucleon collisions, but within the hole-particle or "exciton" formalism, where nucleons are excited from within the Fermi sea, a hole is created. Protons, neutrons, and light fragments are emitted, and the remaining nucleus remains in equilibrium, and specific excitation energy is shared among the remaining nucleons [19].

De-excitation phase: Depending on the mass of the target nucleus and the residual energy, the nucleus can dissipate its residual energy in several ways.

Nuclear evaporation according to the Weisskopf-Ewing approach: here, light particles (alpha, deuteron, triton, etc.) with a kinetic energy of several MeV can be

successively excited from the nucleus and emitted similar to evaporation of a hot system [20].

Fission: the excited nucleus splits into two parts: which only applies to nuclei with high Z (Z≥65). Apart from the implant, nuclei with high Z are not found in the human body and this trend is not significant here.

Fermi breakdown: This mechanism applies to light nuclei (typically A≤16) where the excitation energy of the excited nucleus may exceed the dependence energy of some fragmentation channels. In this case, the excited nucleus disintegrates [21].

B. *Nuclear interactions of heavy ions*

The main difference between nucleus-nucleus and nucleus-nucleon reactions is that the incoming nucleons are not free. This has important phenomenological implications. Most of the models of nucleus-nucleus interactions are related to the "ablation-erosion" model. During the fast phase (ablation), with a time scale of $10^{-23} - 10^{-22}s$, the projectile and the target core collide, resulting in a reaction zone. A quasi-projectile excited with a high initial velocity consists of a quasi-target fragment at rest and several light excited fragments. During the slow phase (erosion, with a time scale of $10^{-18} - 10^{-16}s$, 7 the remaining projectile, target, and light fragments are stimulated through the vaporization of light nuclei or fragments. It should be noted that in this case both the target and the projectile nuclei can be split, while in proton radiation, only target-like nuclei can be fragmented [22-26].

Projectile fragments move further forward, losing energy through ionization and further interactions. These fragments have roughly the same speed and direction as their mothers, but their range is greater than the primary ions because they scale with A / Z^2. Evaporation products from projectile fragments evaporate isotropically in the fragment-projectile frame of reference. The target fragments have a short range and high power, and their vaporization products evaporate isotropically in the target-fragment frame of reference. To describe the dynamic stage of the reaction, various models have been created, which differ mainly in terms of the behavior of the nuclear field affecting the diffusion of particles inside the nucleus [26-30].

Intra-nuclear Cascade Model (INC): This model is related to nuclei with energy higher than 100 MeV/u and has a description similar to that described above for protons. Highly excited nuclei lose energy through a series of two-body reactions and scattering of quasi-free nucleons. More than one nucleon-nucleus interaction can occur in a nucleus-nucleus collision [31-33].

Quantum Molecular Dynamics (QMD): For energies from 50 to about 400 MeV⁄u, this model can be viewed as a complex form of the INC model. Here, each nucleon is described by a Gaussian wave packet, and all nucleons in the projectile and target nuclei participate in the collision process. By minimizing the Hamiltonian that describes the nucleon-nucleon interactions in the projectile and overlapping target nuclei and predicts the formation of heavy or light nuclei and secondary protons and neutrons [34-37].

III. QUANTUM RELATIVISTIC STOPPING POWER AND RANGE FORMULA FOR HADRONS IN HUMAN TISSUES

Ion beams for the treatment of deep tumors (~30 cm) require maximum energy of ~220 MeV for protons and ~430 MeV/u for carbon ions, respectively. The speed of these particles is given by: β_p≈0.6 and βc≈0.7, respectively, therefore, we can use a (semi) relativistic method. In the therapeutic range of energy, ions move through the tissue at these velocities, their energy being reduced mainly by the following two stopping processes:(1) collisional interactions, S_{col} ,

which can result from inelastic Coulomb collisions with orbital electrons of target atoms either inelastic Coulomb collisions with the target atomic orbital electrons atoms, S_{elec}, or interactions by repulsive elastic Coulomb scattering with the atomic nuclei of the target, S_{nuc} and (2): radiative interactions, S_{rad}, due to Bremsstrahlung radiation emission [38]. Thus, the total stopping power of a charged particle is:

$$S = S_{col} + S_{rad} = (S_{elec} + S_{nuc}) + S_{rad} \quad (1)$$

Since the radiative stopping power, S_{rad}, is proportional to the inverse of the square of the projectile mass, therefore, the production of Bremmstrahlung radiation by heavy charged particles is small [39-41]. In radiation therapy, the amount of energy loss due to Coulomb interaction with target nuclei is less than 0.1% of the total stopping power [42], such that this contribution is only related to the energy dissipated caused by projectiles with very low energy below 10 keV/u and in the last few μm of the ion path [42-44]. As a result, the deceleration process is influenced by the electron interaction $S \approx S_{elec}$, which has the highest value at the end of the ion range and causes the release of maximum energy in the selected volume. For ions that move faster than orbital electrons and with charge number Z_p collide with the target material with atomic number Z_t, the amount of energy dissipated per unit length of ion path, $S_{elec}=dE/dx$ is given by Bethe-Bloch formula [42]:

$$\frac{dE}{dx} = \frac{nz^2e^4}{4\pi\varepsilon_0^2 m_e v^2}\left[\left\{\ln\left(\frac{2m_e v^2}{I}\right) + \Delta L_{shell}\right\} L_{Barkas} + \Delta_{LS} - \ln\left(1 - {v^2}/{c^2}\right) - {v^2}/{c^2} - \frac{\delta}{2} + 2ln\gamma - 1 - \frac{1}{\gamma^2}\right. \quad (2)$$

where e is the charge and m_e is the mass of the electron. Also, I is the average ionization energy of the selected material, which varies from about 19 eV for hydrogen to about 820 eV for lead [45]. In high-energy regimes, Fano [45] introduced the last two correction terms of equation 16, which are the density effect correction term, $\frac{\delta}{2}$, and the shell effect correction term, ΔL_{Shell}, respectively. These corrections will be discussed in the following subsections

C. *Density Effect Correction*

Correction of the density effect is a relativistic effect in the stopping power phenomenon, which indicates the reduction of the collision stopping power due to the polarization of the environment, caused by the passage of the charged particle. In dense targets, the field that disturbs the electrons away from the projectile path is modified by the polarization of the dielectric atoms and the electrons away from the projectile [46]. The density effect corrections at high energies have the form: $-\frac{\delta}{2} = -\ln(\beta\gamma) + \ln\left(\frac{1}{\hbar\omega_p}\right) + \frac{1}{2}$, where $\beta=v/c$, $\gamma = \frac{1}{\sqrt{1-\beta^2}}$, $\hbar$ and ω_p are reduced Planck constant, and plasma frequency of the medium, respectively.

D. *Shell Corrections*

Shell corrections occur when the projectile velocity is comparable to the electron velocity of the target atoms. Shell corrections include the following conditions:

1- The speed of the projectile is so low that the inner shell electrons of the target atom have speeds comparable to the projectile.

2- The electrons of the inner shell have a relativistic speed relative to the target atoms that are heavy enough.

Shell correction under the above conditions is: $\Delta L_{Shell} = -\frac{C}{Z}$, where C is defined by the following equation [48]:

$$C = (4.22377 \times 10^{-7}\beta^{-2}\gamma^{-2} + 3.04043 \times 10^{-8}\beta^{-4}\gamma^{-4} - 3.8106 \times 10^{-10}\beta^{-6}\gamma^{-6})I^2 + (3.858019 \times 10^{-9}\beta^{-2}\gamma^{-2} - 1.667989 \times 10^{-10}\beta^{-4}\gamma^{-4} + 1.57955 \times 10^{-12}\beta^{-6}\gamma^{-6})I^3) \quad (3)$$

which is valid for $\beta\gamma$>0.13. I (eV) is the average ionization potential of the target and determines the amount of energy dissipated per unit length of the path. The applicable shell correction, under the second condition, takes into account the total electron binding energy of the ground state of the target atom [49-50]. This correction does not provide any details about the projectile charge role in this situation [51].

E. *Electron Capture*

At low energy (below ~10MeV/u), when the particle velocity is approximately equal to the target electrons' velocity (≈0.0073c), the process of partial ion neutralization (recombination process) due to electron absorption plays an important role in the total stopping power. This process can be entered into the discussed system by replacing z in Eq. 2 with the effective load (z_1) obtained empirically from experimental data by Barkas [52]:

$$Z_{eff}=z\,[1-(125\beta z^{-2/3})]. \quad (4)$$

From the Bethe-Bloch equation, it follows that the inverse of the electronic stopping power is proportional to the square of the particle velocity, and includes the effects of energy straggling and nuclear reactions, which are discussed further.

F. *Barkas correction*

The presence of the Barkas effect has led to the observation of a 0.3% difference with experience in the range of positive and negative pions, which was detected in the nuclear emulsion process [53]. This effect was interesting at the time because it could indicate a difference in the mass of the particle and its antiparticle [54]. More recent measurements confirm the existence of this effect by comparing the stopping power of protons and antiprotons in the keV regime [55]. The Barkas correction accounts for the polarization effect in the target environment due to low-energy collisions between the projectile and distant electrons. If the projectile interacts with a harmonic oscillator, the correction factor $3\pi ze^2\omega\,/\,2m_e v^3$ is obtained [56]. However, from an operational point of view, it is recommended to multiply the original expression of the stopping logarithm, $\ln(2m_e v^2/I)$, by a factor $L_{Baraks}=1+\frac{2z}{\sqrt{Z}}[F(V)]$,here $F(V)=0.0019\exp(-2\ln(\frac{V}{10}))$ and $V=\beta\gamma/\alpha\sqrt{z}$.

Operationally, however, it is recommended to multiply the leading term of the stopping logarithm, $\ln(2m_e v^2/I)$, with the correction: $L_{Baraks}=1+\frac{2z}{\sqrt{Z}}[F(V)]$ where , $F(V)=0.0019\exp(-2\ln(\frac{V}{10}))$ is a ratio of two integrals over a Thomas-Fermi model of the atom. and $V=\beta\gamma/\alpha\sqrt{z}$ is the reduced momentum. Notice that, (V) is not considered reliable below V<0.8. Also the ΔL_{Ls} term in Eq.2 is called Lindhard-Sørensen correction, which is explained below.

G. *Lindhard-Sørensen Correction*

It is important to introduce the Lindhard-Sørensen (LS) correction in the Bloch [57], Mott [58], and Ahlen [59] models, which are collectively called the BMA group due to their common field of study. So that entering this correction expression leads to a more accurate stopping power calculation. The Bloch correction was proven by Felix Bloch in examining the similarities and differences between classical and off of highly charged nuclei. Ahlen's correction is used in Bloch's model in high charge and energy regimes [60]. The Lindhard-Sørensen correction includes the Bloch correction in the low-energy regime, while Mott scattering is a relativistically correct manner [61]:

$$\Delta_{LS}=\sum_{k=1}^{\infty}\Big[\frac{k}{\eta^2}\frac{k-1}{2k-1}sin^2(\delta_k-\delta_{k-1})+\frac{k}{\eta^2}\frac{k+1}{2k+1}sin^2(\delta_{-k}-\delta_{-k-1})+\frac{k}{4k^2-1}\frac{1}{\gamma^2k^2+\eta^2}-\frac{1}{k}\Big]+\frac{\beta^2}{2} \quad (5)$$

In Eq.5, $\eta=\alpha z/\beta$ is a dimensionless parameter with $\alpha=e^2/4\pi\varepsilon_0\hbar c$ which is

called the fine structure constant. $\delta_k$is called the relativistic Coulomb phase shit. While the index k represents the quantum number of angular momentum (including spin).

H. *Finite Nuclear Size Correction*

The finite nuclear size correction includes the physical size of the atomic nuclei in the target environment [62]. This correction is possible because a mathematical description can be given for any spherically symmetric potential [63]. This correction is seen as a correction in the Coulomb phase shift, δ_k, in Eq. 5. This phase shift provides a connection between the internal (nuclear) uniform spherical potential and the external Coulomb potential [64]. We can give a standard function, L_{stand} , which introduces a quantum mechanical perturbation equation,

$$L_{stand} = ln(\frac{2mv^2}{I}\gamma^2) - \frac{v^2}{c^2} - \frac{1}{2}\delta \qquad (6)$$

Such that :$\gamma^2 = (1 - \frac{v^2}{c^2})^{-1}$.In addition, I is determined by Bethe's result, $Z_2 lnI = \sum_n f_{n0} ln(\hbar|\omega_{no}|)$, and estimated by dipole oscillator strengths f_{n0} and transition frequencies ω_{no} . The expression $-\frac{1}{2}\delta$ is the familiar Fermi density effect correction [65], which corrects the adiabatic limit for distant collisions and sufficiently large γ values. The L_{stand} expression in Eq.6 depends only on the particle velocity, v, on the atomic number Z_2 of the environment, and on the mean electron density, n, as included in the density effect. Hence, it does not depend on the particle charge number Z_1, and L_{stand} term introduces the relativistic first-order of quantum perturbation theory, such that $\frac{dE}{dx} \propto Z_1^2$ .The relativistic increase of L_{stand} is included in $ln\gamma^2 - \frac{v^2}{c^2}$and has equipartition, i.e., exactly equal contributions, $ln\gamma - \frac{v^2}{2c^2}$, caused by far and near collisions. But the increase due to distant collisions will be saturated by the density effect correction, $-\frac{1}{2}\delta$, for sufficiently large g. There remains only ln g from close collisions in the relativistic increase of L_{stand}. For simplicity, we have omitted one term belonging to first-order perturbation theory, i.e., the small shell correction due to the finite orbital velocities of the target electrons. The full term belonging to first-order quantum perturbation theory is therefore : $L_{Pert} = L_{stand} + \delta L_{Shell}$. In Eq.6 we have removed the Mott term, which is proportional to $Z_1\frac{v}{c^2}$, and basically belonging to higher-order scattering theory. (Z_1 and Z_2 are projectile particle atomic numbers and target matter, respectively).

IV. Absorbed Dose

The absorbed dose, D, in a given volume, represents the statistical mean of energy absorbed per unit mass of the target at a specific point. It is given by the International Commission on Radiation Units and Measurements (ICRU) as the mean energy (of several energy deposition events from electronic and nuclear interactions), $d\epsilon$, imparted by ionizing radiation in a mass elementdm, in SI units [67]:

$$D=\frac{d\epsilon}{dm}[\frac{J}{kg} = Gray(Gy)] \qquad (7)$$

The physical equation of radiotherapy is the relationship between the absorbed dose, the initial beam current and the mass stopping power: $\frac{1}{\rho}S = -\frac{1}{\rho}\frac{dE}{dx}$. In this regard, for a mono-energetic parallel beam with particle fluence φ passing through a thin slice of material of density ρ, the absorbed dose is expressed as:

$$D[Gy] = \varphi\frac{S}{\rho} = 1.6 \times 10^{-10} \times \varphi\left[\frac{1}{cm^2}\right] \times \frac{dE}{dx}\left[\frac{MeV}{cm}\right] \times \frac{1}{\rho}\left[\frac{cm^3}{g}\right] \qquad (8)$$

V. Energy and Range Straggling

Clinical ion beams are composed of millions (or more) of accelerated ions experiencing different rates of interactions with the matter, therefore most of the physical features that describe them are inherently statistical. The effect of these statistical fluctuations is

discussed as follows. It is often assumed that the rate of energy loss occurs by ions slowing down smoothly and continuously, i.e. in a Continuous Slowing-Down Approximation (CSDA) [66]. Under this assumption, neglecting any stochastic variation, the total ion penetration depth within the absorber may be calculated as:

$$R_{\mathrm{CSDA}}(E) = \int_0^{E_0} \frac{dE}{S} = \int_0^{E_0} \left(\frac{dE}{dx}\right)^{-1} dE \qquad (9)$$

where E_0 is the initial particle kinetic energy. The average range, R_{mean}, is known as the depth at which half of the initial particles have come to rest. Especially in the case of heavy ions, $(E) \approx R_{mean}$, due to the minimal deviations along its trajectory. In order to provide more complete physical concepts about the absorbed dose in different human tissues which are given in Table 1, for the first time we calculated the behavior of the three-dimensional variations of all the terms in Eq.2 such as the effective atomic number, z_{eff} , $\beta = \frac{v}{c}$ parameter, the density effect, $\frac{\delta}{2}$, the shell effect, ΔL_{shell} , Barkas effect, L_{Barkas} , Lynard Sorensen, effect, ΔL_{LS} , the standard perturbation function, L_{stand}, the first-order of the general term of quantum perturbation theory, L_{Pert}, in terms of proton and carbon beam energy and depth of penetration in the different human tissues using Maple programming, and the results are presented in figures 3 to 14. As can be seen from these graphs, because the physical and chemical properties of carbon and hydrogen ions are not the same and carbon is heavier than hydrogen, carbon ion, and hydrogen ion graphs in hadron therapy do not have the same behavior in different body tissues [67].

Table **1** Constants of matter and compositions considered in the evaluation of compounds and mixtures. Compositions of different human tissues are taken from ICRU Report 44 (1989). These values are given for the average ratio of an atomic number to mass Z/A, average excitation energy I, and density ρ.

Material	**<Z/A>**	**I(eV)**	**Density($\frac{g}{cm^3}$)**
Adipose Tissue (ICRU-44)	0.555790	64.80	9.5000E-01
Air, Dry (near sea level)	0.499190	85.70	1.2050E-03
B-100 Bone-Equivalent Plastic	0.527400	85.90	1.4500E+00
Blood, Whole (ICRU-44)	0.549990	75.20	1.0600E+00
Bone, Cortical (ICRU-44)	0.514780	112.00	1.9200E+00
Brain, Grey/White Matter (ICRU-44)	0.552390	73.90	1.0400E+00
Breast Tissue (ICRU-44)	0.551960	70.30	1.0200E+00
Eye Lens (ICRU-44)	0.547090	74.30	1.0700E+00
Lung Tissue (ICRU-44)	0.550480	75.20	1.0500E+00
Muscle, Skeletal (ICRU-44)	0.550000	74.60	1.0500E+00
Ovary (ICRU-44)	0.551490	75.00	1.0500E+00
Water, Liquid	0.555080	75.00	1.0000E+00

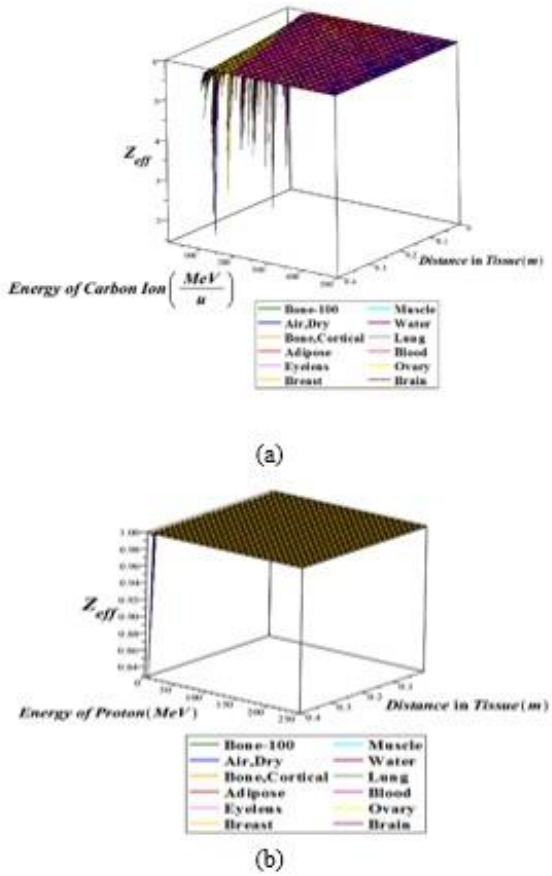

Fig. **3** 3D variations of z_{eff} versus energy and penetration depth for: a) C and b) P in different human tissues

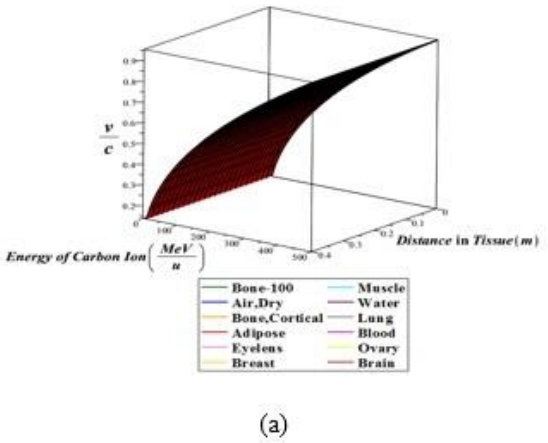

(a)

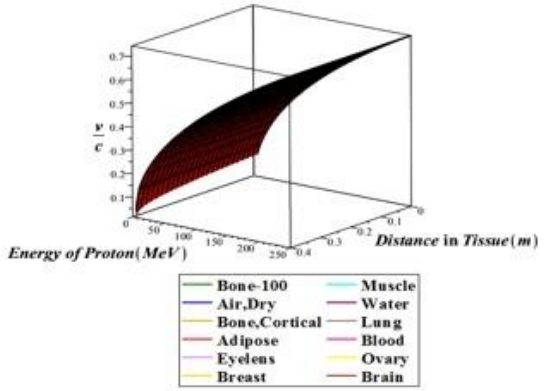

(b)

Fig. **4** 3D variations of $\beta = \frac{v}{c}$ versus energy and penetration depth for: a) C and b) P in different human tissues

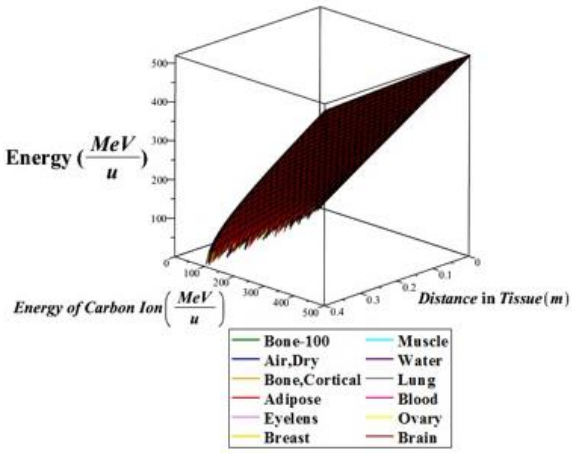

(a)

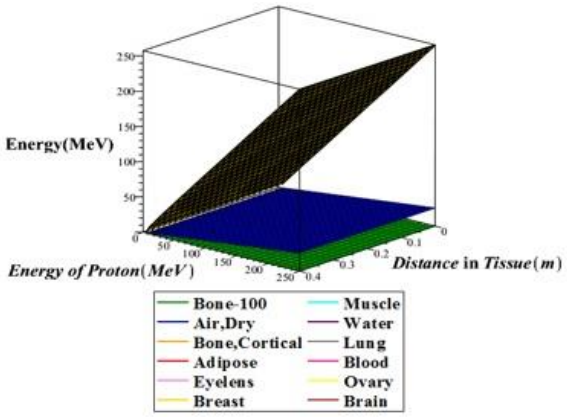

(b)

Fig. **5** 3D variations of hadron energy versus energy and penetration depth for a) C and b) P in different human tissues

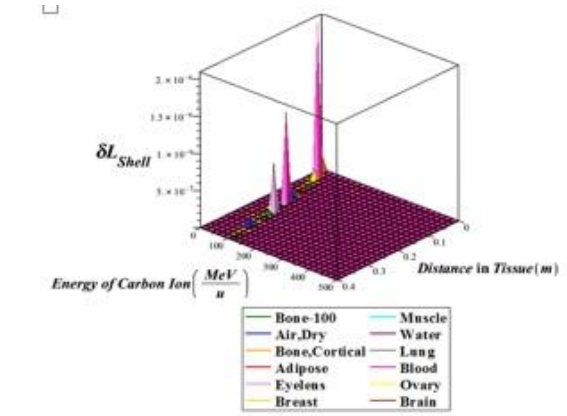

(a)

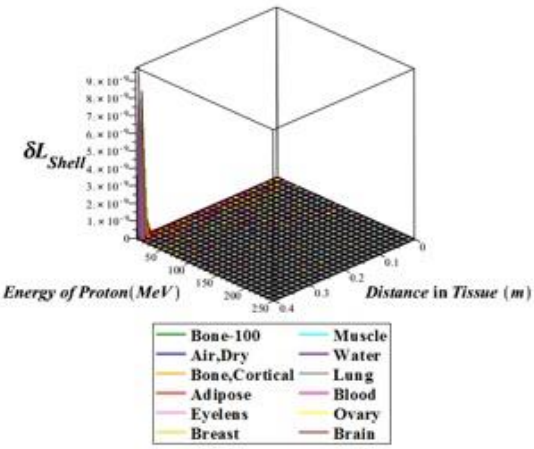

(b)

Fig. **6** 3D variations of δL_{shell} versus energy and penetration depth for: a) C and b) P in different human tissues

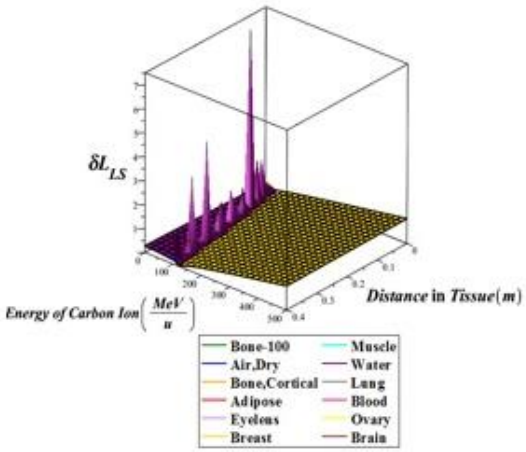

(a)

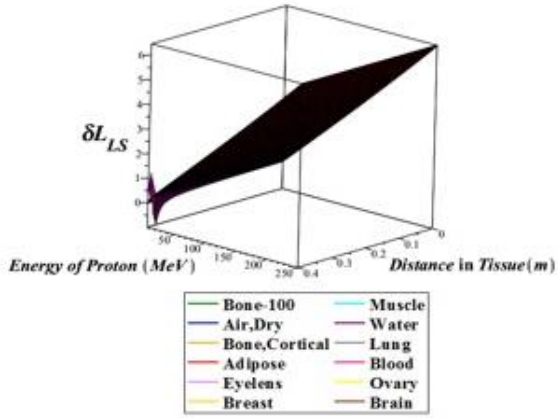

(b)

Fig. **7** 3D variations of δL_{LS} versus energy and penetration depth for: a) C and b) P in different human tissues.

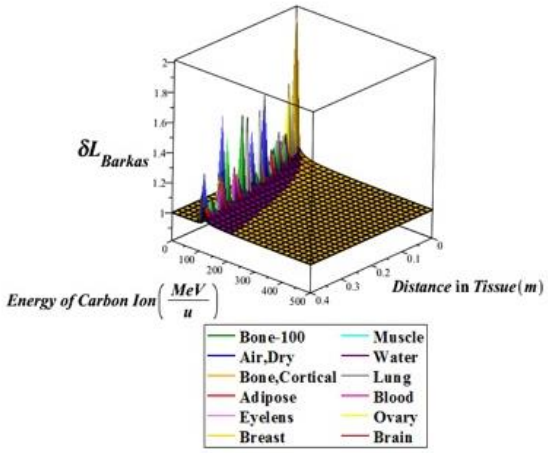

(a)

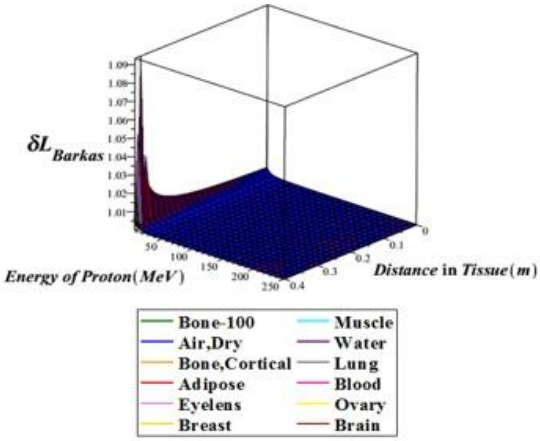

(b)

Fig. **8** 3D variations of δL_{Barkas} versus energy and penetration depth for a) C and b P in different human tissues.

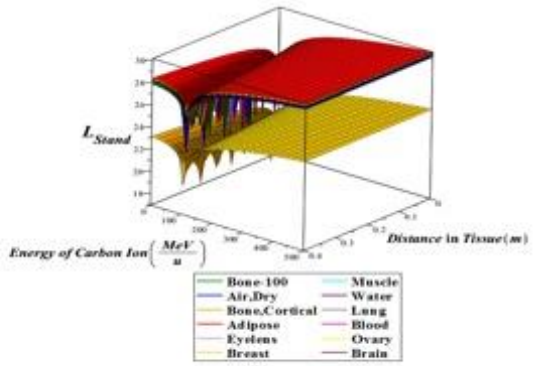

(a)

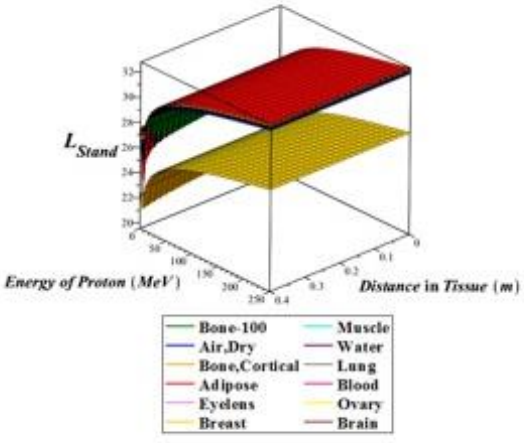

(b)

Fig. **9** 3D variations of L_{stand} versus energy and penetration depth for: a) C and b) P in different human tissues

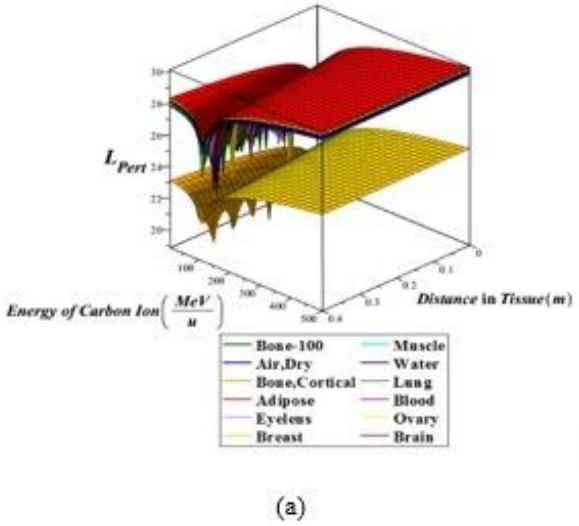

(a)

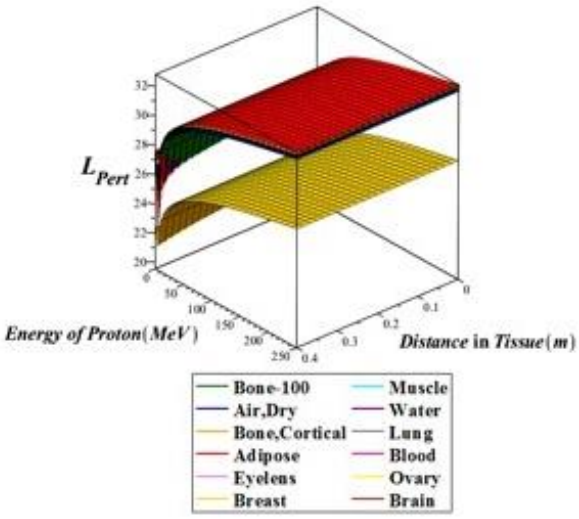

(b)

Fig. **10** 3D variations of L_{pert} versus energy and penetration depth for a) C and b) P in different human tissues

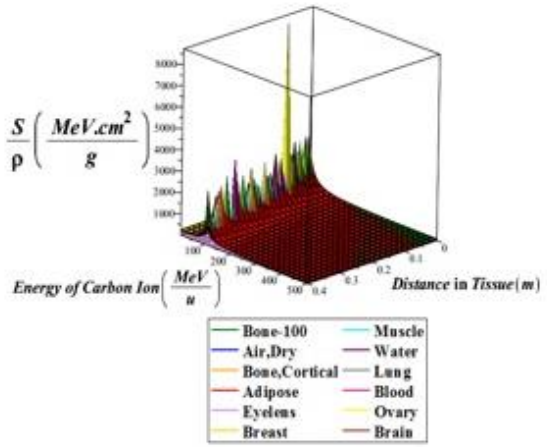

(a)

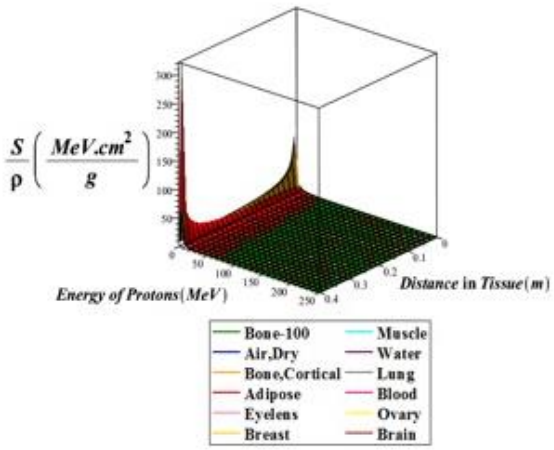

(b)

Fig. **11** 3D variations of $\frac{S}{\rho}$ versus energy and penetration depth for a) C and b) P in different human tissues

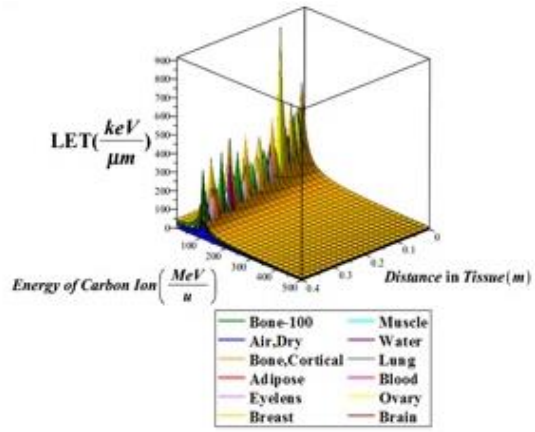

(a)

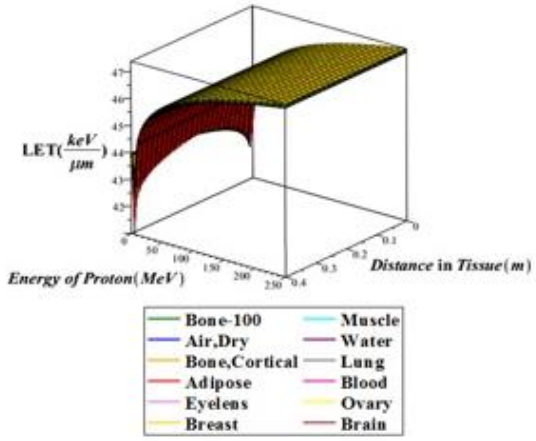

(b)

Fig. **12** 3D variations of *LET* versus energy and penetration depth for a) C and b) P in different human tissues.

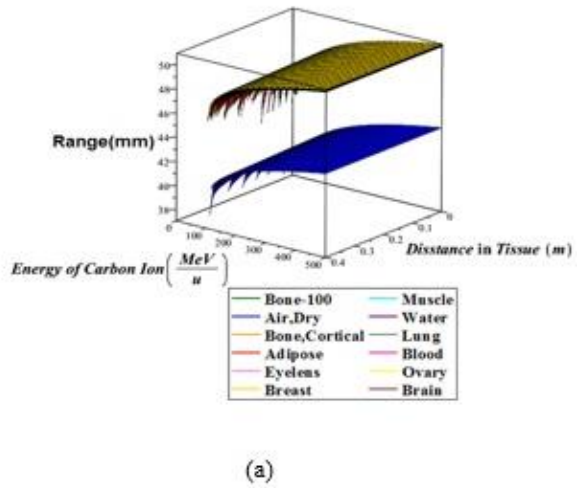

(a)

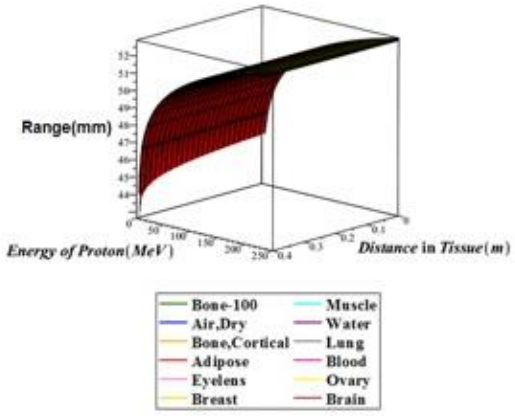

(b)

Fig. **13** 3D variations of $Range$ versus energy and penetration depth for a) C and b) P in different human tissues.

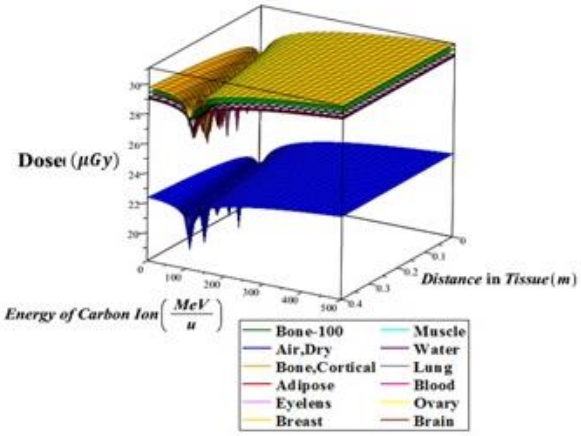

(a)

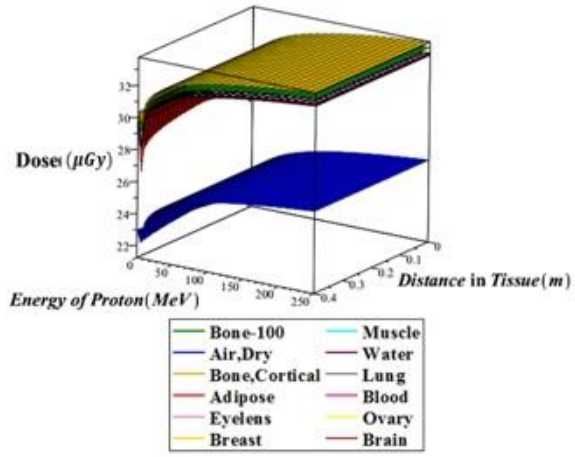

(b)

Fig. **14** 3D variations of $Dose$ versus energy and penetration depth for a) C and b) P in different human tissues.

Now we make a comparison between our work and other research groups. At the energy of 50 MeV, the maximum absorbed dose in the eye lens in our work is 29 Gy, which is in good agreement with the maximum absorbed dose calculated in reference [68] at the same energy (27 Gy). In references [69-71], the absorbed dose in the lung tumor by a proton beam is in the range of (5-60) Gy, which is consistent with our calculation range for lung cancer by a proton beam. In reference [72], carbon therapy of lung cancer has been studied and their results estimated the absorbed dose to be around 20 Gy, while we have obtained around 26 Gy in this work. Also, in reference [73], the average range of the proton at the energy of 100 MeV is about 70 mm, and in water, which in our work is about 50 mm at the same energy; it seems that this difference is because we consider quantum phenomena. We have meant stopping power. Also, our study shows that the absorption dose of carbon is higher than that of a proton in muscle, which is consistent with the results of reference [74].

In the reference [75], carbon therapy of breast cancer has been studied and their results have obtained the absorbed dose of about 36Gy, while we have estimated about 30Gy in this work. By looking at reference [76], it can be seen that the LET amount in water for a

proton with an energy of 200 MeV is about 45 keV⁄μm, while for carbon with an energy of 391 MeV⁄u, it is about 11.17 keV⁄μm. In our calculation results, for a proton with an energy of 200 MeV, the LET amount is about 46.1keV⁄μm, and for carbon with an energy of 391 MeV⁄u, it is about 10.23keV⁄μm. it can be concluded that our results are in good agreement with the results of this reference.

VI. Conclusion

Hadron therapy with heavy charged particles is considered to be a modern technique in current radiation therapy, the reasons for which can be found in its physical and radiobiological advantages and their set of clinical properties. Physically, due to the optimal dose distribution of heavy charged particles, it is possible to protect healthy tissues from unwanted damage to a significant extent, which in turn reduces side effects and secondary cancers. In addition, from a radiobiological point of view, these particles have a higher RBE compared to photons, thus increasing the efficiency of destroying cancer cells and increasing the possibility of tumor control. Thus, this technique is the preferred method for cancer treatment. In this work for the first time, we study the relativistic theory of hadron therapy with carbon and proton. In the years that have passed since the beginning of hadron therapy, the demand for using this treatment method has been increasing. The conducted studies show that during the years that have passed since the invention of this method, each of the mentioned parts has undergone transformation and a relative improvement in the safety and accuracy of dose delivery has been achieved in order to improve the quality of treatment.

On the other hand, the high cost of treatment compared to traditional radiation therapy, the high cost of equipment and their maintenance has been an important challenge in the lack of development of such centers around the world. Therefore, it is hoped that in the coming years, with the reduction of costs, the possibility of the development and utilization of hadron therapy centers around the world will be provided.

References

[1] C.A. Tobias, H.O. Anger, and J.H. Lawrence, “Radiological use of high energy deuterons and alpha particles,” Am J Roentgenol Radium Ther Nucl Med, vol. 67, pp. 1–27, 1952.

[2] S.B. Curtis, “Plans for the high-energy, heavy-ion facility (BEVALAC) at Berkeley,” Eur J Cancer, vol. 10, pp. 388, 1974.

[3] J.R. Castro, J.M. Quivey, J.T. Lyman, G. Chen, T.L. Phillips, and C.A. Tobias, “Radiotherapy with heavy charged-particles at Lawrence Berkeley Laboratory,” J Can Assoc Radiol, vol. 31, pp. 30 - 4, 1980.

[4] H. Tsujii and T. Kamada, “A review of update: clinical results of carbon ion radiotherapy,” Jpn J Clin Oncol, vol. 42, pp. 670-685, 2012.

[5] T. Kanai, Y. Furusawa, K. Fukutsu, H. Itsukaichi, K. Eguchi-Kasai, and H. Ohara, “Irradiation of mixed beam and design of spread-out Bragg peak for heavy-ion radiotherapy.” Radiat Res, 147, pp. 78–85, 1997.

[6] N. Hamada, T. Imaoka, S. Masunaga, T. Ogata, R. Okayasu, A. Takahashi, T.A. Kato, Y. Kobayashi, T. Ohnishi, K. Ono, Y. Shimada, and T. Teshima, “Recent advances in the biology of heavy-ion cancer therapy.” J Radiat Res, 51, pp. 365–383, 2010.

[7] W.K. Weyrather, S. Ritter, M. Scholz, and G. Kraft, “RBE for carbon track-segment irradiation in cell lines of differing repair capacity,” Int J Radiat Biol, vol. 75, pp.1357–1364, 1999.

[8] T. Kanai, M. Endo, S. Minohara, N. Miyahara, H. Koyama-ito, H. Tomura, N. Matsufuji, Y. Futami, A. Fukumura, T. Hiraoka, Y. Furusawa, K. Ando, M, Suzuki, and F. Soga, “Biophysical characteristics of HIMAC clinical irradiation system for heavyion radiation therapy,” Int J Radiat Oncol Biol Phys, vol. 44, pp. 201–210, 1999.

[9] K. Ando and Y. Kase, "Biological characteristics of carbon-ion therapy," Int J Radiat Biol, vol. 85, pp. 715–728, 2009.

[10] T. Ogata, T. Teshima, K. Kagawa, Y. Hishikawa, Y. Takahashi, A. Kawaguchi, Y. Suzumoto, K. Nojima, Y. Furusawa, and N. Matsuura, "Particle irradiation suppresses metastatic potential of cancer cells," Cancer Res, vol. 65, pp. 113–120, 2005.

[11] HW. Lewis, "Multiple scattering in an infinite medium," Phys Rev, vol. 78, pp. 526–535, 1950.

[12] VL. Highland, "Some practical remarks on multiple scattering," Nucl Instrum Methods, vol. 129, pp. 497–506, 1975.

[13] B. Gottschalk, "On the scattering power of radiotherapy protons," Med Phys, vol. 37, pp. 352–67,2010.

[14] S. G. Mashnik, K. K. Gudima, R. E. Prael, A. J. Sierk, M. I. Baznat, and N. V. Mokhov, "CEM03.03 and LAQGSM03.03 Event Generators for the MCNP6, MCNPX, and MARS15 Transport Codes," February 4–8, ICTP, Trieste, Italy. arXiv:0805.0751, 2008.

[15] A.Ferrar and PR.Sala, "The physics of high energy reactions," Proceed Workshop on Nucl. Reaction Data and Nuclear Reactor Physics, Design and Safety, Vol. 2, pp. 424–532, 1998.

[16] R.Serber, "Nuclear reactions at high energies," Phys Rev, vol. 72, pp.1114–1119, 1947.

[17] H. W. Bertini, T. A. Gabriel, R. T. Santoro, 0. W. Hermann, N. M. rson, and J. M. Hunt, "HIC-1: A First Approach to the Calculation of Heavy-Ion Reactions at Energies50 MeV/Nucleon," Oak Ridge: ORNL-TM-vol. 4134, pp. 1-54, 1974.

[18] JJ.Griffin, "Statistical model of intermediate structure," Phys Rev Lett1, vol. 7, pp. 478–80, 1966,

[19] M. Blann, "Precompound analyses of spectra and yields following nuclear capture of stopped pi-," Phys Rev, pp. 1648-1662, 1983.

[20] VF.Weisskopf, "Statistics and nuclear reactions," Phys Rev, vol. 52, pp. 295–303, 1937.

[21] E.Fermi, "High energy nuclear events," Progr Theor Phys, vol. 5, pp. 570–83, 1950.

[22] D.Cussol, "Nuclear Physics and Hadron Therapy," La Colle sur Loup: Lectures at Ecole Joliot Curie, vol. 46, pp.1-47, 2011.

[23] E. Pedroni, S. Scheib, T. Böhringer, A. Coray, M. Grossmann, S. Lin, and A Lomax, "Experimental characterization and physical modelling of the dose distributionof scanned proton pencil beams," Phys Med Biol, vol. 50, pp. 541–561, 2005.

[24] G. O Sawakuchi, U. Titt, D. Mirkovic, G. Ciangaru, X R. Zhu, N. Sahoo, M. T Gillin, and R. Mohan, "Monte Carlo investigation of the low-dose envelope from scanned proton pencil beams," Phys Med Biol, vol. 55, pp. 711–721, 2010.

[25] B. Gottschalk, *Physics of proton interactions in matter*, CRC Press, 2018.

[26] M. Krämer, M. Durante, "Ion beam transport calculations and treatment plansin particle therapy," Eur Phys J D, vol. 60, pp. 195–202, 2010.

[27] C. Labaune, C. Baccou, S. Depierreux, C. Goyon, G. Loisel, V. Yahia, and J. Rafelski, "Fusion reactions initiated by laser-accelerated particle beams in a laser-produced plasma," Nature Communications, vol. 4, pp. 2506 (1-6), 2013.

[28] J. M. Martinez-Val, S. Eliezer, M. Piera, and G. Velarde, "Fusion burning waves in proton-boron-11 plasmas," Phys. Lett. A, vol. 216, pp. 142-152, 1996.

[29] D. C. Moreau, "Potentiality of the proton-boron fuel for controlled thermonuclear fusion," Nucl. Fusion, vol. 17, pp. 13-20, 1977.

[30] B. Levush and S. Cuperman, "On the potentiality of the proton-boron fuel for inertially confined fusion," Nucl. Fusion, vol. 22, pp. 1519-1525, 1982.

[31] T. Kobayashi, Y. Sakurai, and M. Ishikawa, "A noninvasive dose estimation system for clinical BNCT based on PG-SPECT--conceptual study and fundamental experiments using HPGe and CdTe semiconductor detectors," Med. Phys, vol. 27, pp. 2124-2132, 2000.

[32] D.Yoon, J.Jung, and T. Suha, "Application of proton boron fusion reaction to radiation therapy: A Monte Carlo simulation study," APPLIED PHYSICS LETTERS, vol. 105, pp. 223507(1-12), 2014.

[33] L. Giuffrida, D. Margarone, G.A.P. Cirrone, A. Picciotto, and G. Korn, "Prompt gamma ray diagnostics and enhanced hadron-therapy using neutron free nuclear reactions," AIP ADVANCES, vol. 6, pp. 105204 (1-18), 2016.

[34] S.Eliezer, H. Hora, G.Korn, N.Nissim, and J. M.Martinez, "Avalanche proton-boron fusion based on elastic nuclear collisions," Physics of Plasmas, vol. 23, pp. 050704 (1-4), 2016.

[35] H. Hora, G. Korn, L. Giuffrida, D. Margarone, A. Picciotto, J. Krasa, K. Jungwirth, J. Ullschmied, P. Lalousis, Sh. Eliezer, G. H. Miley, S. Moustaizis, and G. Mourou, "Fusion energy using avalanche increased boron reactions for block-ignition by ultrahigh power picosecond laser pulses," Laser and Particle Beams, vol. 33, pp. 607–619, 2015.

[36] U. Amaldi and S. Braccini, "Present challenges in hadron therapy techniques," Eur Phys J Plus, vol. 126, pp. 70-85, 2011.

[37] D. Schulz-Ertner, O. Jäkel, W. Schlegel, and W. Schlegel, "Radiation therapy with charged particles," Semin Radiat Oncol, vol. 16, pp. 249-259, 2006.

[38] W. R. Leo, *Techniques for Nuclear and Particle Physics Experiments*, Springer-Verlag, 2nd Ed edition, 1990.

[39] F. H. Attix, *Introduction to Radiological Physics and Radiation Dosimetry*, WILEY-VCH Verlag GmbH & Co, KGaA, Weinheim, 1986.

[40] W. D. Newhauser and R. Zhang, "The physics of proton therapy," Physics in Medicine and Biology, vol. 60, pp. 155, 2015.

[41] W. R. Leo, Techniques for Nuclear and Particle Physics Experiments, Springer-Verlag, 2nd Ed edition, 1990.

[42] J. F. Ziegler, "The Stopping of Energetic Light Ions in Elemental Matter," J.Appl. Phys/Rev. Appl.Phys, vol. 85, pp. 1249–1272, 1999.

[43] D. Schardt and T. Elsässer, "Heavy-ion tumor therapy: Physical and radiobiological benefits," ReviewsofModernPhysics, vol. 82, pp. 383–425, 2010.

[44] A.C. Kraan, "Range Verification Methodsin Particle Therapy: Underlying Physicsand Monte Carlo Modeling," Frontiers in Oncology, vol. 5, pp. 150-177, 2015.

[45] U. Fano, *Penetration of protons, alpha particles and mesons*, National Bureau of Standards, 1963.

[46] E. Fermi, "The Ionization Loss of Energy in Gases and in Condenses Materials," Physical Review, vol. 57, pp. 485-493, 1940.

[47] U. Fano, "Penetration of Protons, Alpha Particles, and Mesons," Annual Review of Nuclear Science, vol. 13, pp. 1-66, 1963.

[48] H. Bichsel, *Passage of charged particles through matter*, 3rd Ed, New York, McGraw-Hill, 1972.

[49] P. T. Leung, "Bethe stopping-power theory for heavy-target atoms," Physical Review A, vol. 40, pp. 5417-5419, 1989.

[50] P.T. Leung, "Addendum: Bethe stopping-power theory for heavy-target atoms," Physical Review A, vol. 60, pp. 2562-2564, 1999.

[51] B.A. Weaver and A.J. Westphal, "Energy loss of relativistic heavy ions in matter," Nucl. Instrum. Methods Phys. Res. B, vol. 187, pp. 285-301, 2002.

[52] W.H. Barkas, J.N. Dyer, and H.H. Heckman, "Errata: Resolution of the Σ^--Mass Anomaly," Physical Review Letters, vol. 11, pp. 138-145, 1963.

[53] F.M. Smith, W. Birnbaum, and W.H. Barkas, "Measurements of Meson Masses and Related Quantities," Physical Review, vol. 91, pp. 765-766, 1953.

[54] W.H. Barkas, J.N. Dyer, and H.H. Heckman, "Resolution of the Σ^-Mass Anomaly," Physical Review Letters, vol. 11, pp. 26-28, 1963.

[55] R. Medenwaldt, S.P. Møller, E. Uggerhøj, and T. Worm, "Measurement of the stopping power of silicon for antiprotons between 0.2 and 3 MeV," Nuclear Instruments and Methods in Physics Research Section B: Beam Interactions with Materials and Atoms, vol. 58, pp. 1-5, 1991.

[56] J. Lindhard, "The Barkas Effect - or Z3, Z4-Corrections to Stopping of Swift Charged

Particles," Nuclear Instruments and Methods, vol. 132, pp. 1-5, 1976.

[57] F. Bloch, "Zur Bremsung rasch bewegter Teilchen beim Durchgang durch Materie," Annalen der Physik,vol. 16, pp. 285-320, 1933.

[58] S.P. Ahlen, "Theoretical and experimental aspects of the energy loss of relativistic heavily ionizing particles," Reviews of Modern Physics, vol. 52, pp. 121-173, 1980.

[59] S.P. Ahlen, "Calculation of the relativistic Bloch correction to stopping power," Physical Review A, vol. 25, pp. 1856-1867, 1982.

[60] S.P. Ahlen and G. Tarlé, "Observation of Large Deviations from the Bethe-Bloch Formula for Relativisitic Uranium Ions," Physical Review Letters, vol. 50, pp. 1110-1113, 1983.

[61] J. Lindhard, A.H. Sørensen, "Relativistic theory of stopping for heavy ions," Physical Review A, vol. 53, pp. 2443-2456, 1996.

[62] S. Datz, H.F. Krause, C.R. Vane, H.V. Knudsen, P. Grafström, R.H. Schuch, "Effect of Nuclear Size on the Stopping Power of Ultrarelativistic Heavy Ions," Physical Review Letter ,vol. 77, pp. 2925-2928, 1996.

[63] M.E. Rose, *Relativistic Electron Theory,* New York, Wiley, 1961.

[64] C.P. Bhalla and M.E. Rose, "Finite Nuclear Size Effects in β Decay," Physical Review, vol. 128, pp. 774-778, 1962.

[65] E. Fermi, "The Ionization Loss of Energy in Gases and in Condensed Materials," Phys. Rev. vol. 57, pp. 485-494,1940.

[66] M.J. Berger and S.M. Seltzer, "Tables of Energy Losses and Ranges of Electrons and Positrons," Nasa Sp. Vol. 3012, pp. 1–134, 1964.

[67] DJ Thomas, "ICRU85. ICRU Report 85a - Fundamental Quantities And Units For Ionizing Radiation," Journal of the ICRU, vol. 11, pp.1–35, 2011.

[68] Sh. Safaiean, M. Salehi Barough, and S. P. Shirmardi,"calculation of brain and thyroid radiation scattered absorbed dose due to proton therapy of eyes using MCNPX simulation code," New Cellular and Molecular Biotechnology Journal, vol. 10, pp. 29-40, 2020.

[69] T. Ohno, Y. Oshiro, M. Mizumoto, H. Numajiri, H. Ishikawa, T. Okumura, T. Terunuma, T. Sakae, and H. Sakurai, "Comparison of Dose-Volume Histograms Between Proton Beam and X-Ray Conformal Radiotherapy for Locally Advanced Non-Small-Cell Lung Cancer," Journal of Radiation Research, vol. 56, pp. 128–133, 2015.

[70] R. Charles Nichols, S. N. Huh, R. H. Henderson, N. P. Mendenhall, S. Flampouri, Z. Li, H. J. D'Agostino, J. D. Cury, D. C. Pham, and B. S. Hoppe, "Proton Radiation Therapy Offers Reduced Normal Lung and Bone Marrow Exposure for Patients Receiving Dose-Escalated Radiation Therapy for Unresectable Stage III non-Small-Cell Lung Cancer: A Dosimetric Study," Clin Lung Cancer, vol. 12, pp. 252-257, 2011.

[71] N. Kubo, J-i Saitoh, Hirofumi Shimada, Katsuyuki Shirai, Hidemasa Kawamura, T. Ohno, and T. Nakano, "Dosimetric Comparison of Carbon Ion and X-Ray Radiotherapy for Stage IIIA Non-Small Cell Lung Cancer," J Radiat Res. Vol. 57, pp. 548–554, 2016.

[72] C. D. Schlaff, A. Krauze, A. Belard , J. J. Connell and K. A. Camphause ," Bringing the heavy: carbon ion therapy in the radiobiological and clinical context," Radiation Oncology, vol. 57, pp. 548–554, 2014.

[73] M. Ebrahimi Loushab, A.A. Mowlavi, M.H. Hadizadeh, R. Izadi, and S.B. Jia,"Impact of Various Beam Parameters on Lateral Scattering in Proton and Carbon-ion Therapy" J Biomed Phys Eng. Vol. 5, pp. 169–176, 2015.

[74] H. Noshad, " Monte Carlo computation of dose deposited by

[75] carbon ions in radiation therapy," Iran. J. Radiat. Res. vol. 4, pp.115-120, 2006.

[76] X. Wang , X. Chen , G. Li , X. Han , T. Gao , W. Liu, and Xi. Tang," Application of Carbon Ion and Its Sensitizing Agent in Cancer Therapy: A Systematic Review," Frontiers in Oncolog, vol. 11, pp. 708724 (1-21), 2021.

[77] M. Rovituso and C. La Te," Nuclear interactions of new ions in cancer therapy: impact on

[78] dosimetry,"Transl Cancer Res. vol. 6, pp. 1-20, 2017.